Atomic and molecular intracules for excited states

Nicholas A. Besley[a] and Peter M. W. Gill
School of Chemistry, University of Nottingham, University Park, Nottingham, NG7 2RD, United Kingdom

Intracules in position space, momentum space and phase space have been calculated for low-lying excited states of the He atom, Be atom, formaldehyde and butadiene. The phase-space intracules (Wigner intracules) provide significantly more information than the position- and momentum-space intracules, particularly for the Be atom. Exchange effects are investigated through the differences between corresponding singlet and triplet states. © *2004 American Institute of Physics.*
[DOI: 10.1063/1.1690233]

I. INTRODUCTION

Much of modern electronic structure theory is based on the one-electron density $\rho(\mathbf{r})$. The relative simplicity of $\rho(\mathbf{r})$ compared to the many electron wave function $\Psi(\mathbf{r}_i)$ leads to computationally cost effective methods. Furthermore, chemically useful information can be more easily gleaned from $\rho(\mathbf{r})$. However, this simplicity comes at a price, and when $\Psi(\mathbf{r}_i)$ is reduced to $\rho(\mathbf{r})$ much information is lost. In particular, it is often valuable to retain explicit two-electron information. Intracules are two-electron distribution functions and are an intermediate quantity between $\rho(\mathbf{r})$ and $\Psi(\mathbf{r}_i)$.

The intracule density $I(\mathbf{u})$, represents the probability density for the interelectronic vector $\mathbf{u} = \mathbf{r}_1 - \mathbf{r}_2$:

$$I(\mathbf{u}) = \int \rho_2(\mathbf{r}_1, \mathbf{r}_2) \delta(\mathbf{r}_{12} - \mathbf{u}) d\mathbf{r}_1 d\mathbf{r}_2, \tag{1}$$

where $\rho_2(\mathbf{r}_1, \mathbf{r}_2)$ is the two-electron density. A simpler quantity is the spherically averaged intracule density

$$P(u) = \int I(\mathbf{u}) d\Omega_u, \tag{2}$$

which measures the probability that two-electrons are separated by a *scalar* distance $u = |\mathbf{u}|$.

Position intracules have received considerable attention from a number of authors.[1–37] Much of this work has been concerned with studying the difference between intracules for correlated and uncorrelated wave functions, the so-called Coulomb hole.[2] The moments of position intracules for a large number of atoms based on numerical Hartree–Fock (HF) wave functions have been reported by Koga and Matsuyama.[30,31] More recently, the computation of HF position intracules for large systems has been described and implemented.[33] Molecular position intracules generally have a number of distinct features that correspond to the underlying molecular framework.[35]

Analogous quantities can be defined in momentum space. $\bar{I}(\mathbf{v})$ represents the probability density of a relative momentum vector $\mathbf{v} = \mathbf{p}_1 - \mathbf{p}_2$:

$$\bar{I}(\mathbf{v}) = \int \pi_2(\mathbf{p}_1, \mathbf{p}_2) \delta(\mathbf{p}_{12} - \mathbf{v}) d\mathbf{p}_1 d\mathbf{p}_2, \tag{3}$$

where $\pi_2(\mathbf{p}_1, \mathbf{p}_2)$ is the momentum two-electron density. Similarly the spherically averaged intracule

$$M(v) = \int \bar{I}(\mathbf{v}) d\Omega_v \tag{4}$$

is a measure of the probability that two electrons will have relative momentum $v = |\mathbf{v}|$. We have adopted the notation outlined previously,[38] and $P(u)$ is called the position intracule and its counterpart the momentum intracule is denoted $M(v)$.

Research involving momentum intracules has closely followed that for position intracules.[28,39–59] Much of the early work, including the study of the Coulomb hole, was done by Banyard and co-workers.[39–42,44–47] Molecular HF momentum intracules for relatively large systems have been reported.[59] Generally, these intracules are smooth functions that lack the well-defined structure of their position space counterparts.

Recently, a new joint position *and* momentum intracule, called the Wigner intracule $W(u,v)$, has been defined[38]

$$W(u,v) = \int W_2(\mathbf{r}_1, \mathbf{p}_1, \mathbf{r}_2, \mathbf{p}_2) \delta(\mathbf{r}_{12} - \mathbf{u}) \delta(\mathbf{p}_{12} - \mathbf{v})$$
$$\times d\mathbf{r}_1 d\mathbf{r}_2 d\mathbf{p}_1 d\mathbf{p}_2 d\Omega_u d\Omega_v, \tag{5}$$

where W_2 is the second-order reduced Wigner function[60–62]

$$W_2(\mathbf{r}_1, \mathbf{p}_1, \mathbf{r}_2, \mathbf{p}_2) = \frac{1}{\pi^6} \int \rho_2(\mathbf{r}_1 + \mathbf{q}_1, \mathbf{r}_1 - \mathbf{q}_1, \mathbf{r}_2 + \mathbf{q}_2,$$
$$\mathbf{r}_2 - \mathbf{q}_2) e^{-2i(\mathbf{p}_1 \cdot \mathbf{q}_1 + \mathbf{p}_2 \cdot \mathbf{q}_2)} d\mathbf{q}_1 d\mathbf{q}_2. \tag{6}$$

The Wigner intracule is a measure of the combined probability that electrons are separated by u with relative momentum v. $W(u,v)$ is related to the position and momentum intracules through

$$P(u) = \int_0^\infty W(u,v) dv, \tag{7}$$

a)Electronic mail: nick.besley@nottingham.ac.uk

$$M(v) = \int_0^\infty W(u,v)\,du, \qquad (8)$$

Hartree–Fock $W(u,v)$ have been presented for a number of systems.[38,63] Wigner intracules often have a number of distinct features that can be attributed to interactions between electrons in particular orbitals.[38]

Work involving intracules has generally focused on atoms and molecules in their ground electronic states. However, it is also of interest to examine intracules for electronically excited states since this provides insight into changes in the electronic distribution upon excitation. Both position and momentum intracules for a variety of excited states of He have been studied in detail.[8,10,11,14,16,18,22,28,30,31,42,49,64,65] Part of the motivation for these studies was to examine the Coulomb hole and the difference in intracule density between singlet and triplet states. These difference intracules are related to the Fermi hole[66] and provide insight into the effects of exchange. In early work, position intracules for the singlet and triplet $S(1s2s)$ states of He were reported.[9,64] It was found that the Coulomb hole for the excited states is more complex than the Coulomb hole of the ground state. Katriel[8] showed that for He there is a reduction of the probability of finding electrons close together in the $^3P(1s2p)$ state compared to the corresponding singlet state. However, there is a considerable increase in finding electrons at moderate separation and a reduced probability of large separations. This was consistent with the counter-intuitive observation that the interelectronic repulsion is greater in the higher multiplicity term.[67] The lower energy of the triplet state arises from an increase in the electron-nucleus attraction. It has been noted that the physical origin of this "reverse correlation" behavior is associated with the large size of the $2p$ orbital.[68] Similar observations were found for the $^1\Pi_u$ and $^3\Pi_u$ states of H_2.[11] This behavior was confirmed in a subsequent study[18] in which position intracules were generated for the singlet and triplet $P(1s2p)$ states of He-like ions (He→Mg^{10+}) from accurate correlated wave functions. The increase in interelectronic repulsion on the inclusion of electron correlation was found to decrease as the nuclear charge of the ions increased. In a related study,[16] Regier and Thakkar presented position intracules for the singlet and triplet $S(1s2s)$ and $P(1s2p)$ states of He-like ions. This showed very small interelectronic separations to be more likely in the singlet state due to the presence of the Fermi hole in the triplet state. This tendency increased with the nuclear charge of the ion. Furthermore, both $P(1s2p)$ and $S(1s2s)$ states showed qualitatively similar behavior. It was also suggested that the local maximum found in the intracule for the $^1S(1s2s)$ state arises from the nodal structure of the wave function rather than the absence of the Fermi hole. Position and momentum intracules were reported for the $^1P(1s2p)$ and $^3P(1s2p)$ states of He based on wave functions consisting of a linear combination of Slater determinants.[28] Although derived from less accurate wave functions, the singlet–triplet difference of the position intracule was found to be similar to the near-exact curve presented earlier by Regier and Thakkar.[16] The corresponding momentum intracules showed there to be greater probability of low relative momentum in the singlet state.

TABLE I. Correlation energies (in au) for the lowest triplet states.

System	CIS/6-31+G	CCSD/6-31+G
Be	+0.001	−0.001
Formaldehyde	+0.040	−0.192
Butadiene	−0.016	−0.380

Coulomb holes for excited states of the Be-like ions have been reported,[10] where, as expected, the triplet states generally possess shallower Coulomb holes than the singlet states. Koga, Matsuyama, and co-workers[30,31] studied position and momentum intracules for the group 14, 15, and 16 atoms. States with higher angular momentum were found to have an increased probability of finding pairs of electrons separated by a short distance. Recently,[69] position intracules derived from correlated wave functions have been reported for a number of excited states of Be-like ions. The difference intracules between the singlet and triplet states showed qualitatively different behavior depending on the nuclear charge. The $^1P(2s2p) - {}^3P(2s2p)$ intracule for Be showed a negative region at low u and a positive region at high u. For the ions $C^{2+} \rightarrow Ne^{6+}$ this behavior was reversed, with a positive region at low u. While like Be, B^+ showed a negative region at low u; at long range its behavior differed from Be.

While a limited class of excited states can be studied using HF theory, in order to generate arbitrary excited states it is necessary to go beyond the HF approximation. In this article, we describe the computation of position, momentum, and Wigner intracules for the configuration interaction in the space of all singly excited determinants (CIS) wave function. This allows intracules to be computed for atoms and molecules in electronically excited states for relatively large molecular systems in position, momentum, and phase space. The CIS method contains no description of dynamic electron correlation. This is illustrated by the correlation energies for CIS and coupled cluster (CCSD) wave functions shown in Table I. These show there is only a relatively small energy difference between the HF and CIS wave functions, while the CCSD wave function introduces a significant correction. However, intracules derived from the CIS wave function should be qualitatively similar to those from more exact wave functions. Furthermore, intracules from uncorrelated wave functions can be used to evaluate correlation energies.[70] The computation of intracules for CIS wave functions using Gaussian basis functions within Q-Chem[71] is described. Subsequently, position, momentum, and Wigner intracules for a number of excited states of atomic and molecular systems are presented and discussed. The effects of exchange are also examined in position, momentum, and phase space through the evaluation of the difference intracule densities between singlet and triplet states. Atomic units are used throughout.

II. THEORY

The computation of $P(u)$,[33] $M(v)$,[59] and $W(u,v)$[63] have been described in detail elsewhere, consequently, only a brief description is given here.

If the molecular orbitals are expanded within a basis set

$$\psi_a(\mathbf{r}) = \sum_{\mu}^{N} c_{\mu a}\phi_\mu(\mathbf{r}), \tag{9}$$

the intracules can be expressed as

$$P(u) = \sum_{\mu\nu\lambda\sigma} \Gamma_{\mu\nu\lambda\sigma}(\mu\nu\lambda\sigma)_P, \tag{10}$$

$$M(v) = \sum_{\mu\nu\lambda\sigma} \Gamma_{\mu\nu\lambda\sigma}(\mu\nu\lambda\sigma)_M, \tag{11}$$

$$W(u,v) = \sum_{\mu\nu\lambda\sigma} \Gamma_{\mu\nu\lambda\sigma}(\mu\nu\lambda\sigma)_W, \tag{12}$$

where $\Gamma_{\mu\nu\lambda\sigma}$ is the two-particle density matrix and $(\mu\nu\lambda\sigma)_P$, $(\mu\nu\lambda\sigma)_M$, and $(\mu\nu\lambda\sigma)_W$ are the position, momentum, and Wigner integrals, respectively:

$$(\mu\nu\lambda\sigma)_P = \int \phi_\mu(\mathbf{r})\phi_\nu(\mathbf{r})\phi_\lambda(\mathbf{r}+\mathbf{u})\phi_\sigma(\mathbf{r}+\mathbf{u})d\mathbf{r}d\Omega_u, \tag{13}$$

$$(\mu\nu\lambda\sigma)_M = \frac{v^2}{2\pi^2}\int \phi_\mu(\mathbf{r})\phi_\nu(\mathbf{r}+\mathbf{q})\phi_\lambda(\mathbf{q}+\mathbf{u})\phi_\sigma(\mathbf{u})$$
$$\times j_0(qv)d\mathbf{r}d\mathbf{q}d\mathbf{u}, \tag{14}$$

$$(\mu\nu\lambda\sigma)_W = \frac{v^2}{2\pi^2}\int \phi_\mu(\mathbf{r})\phi_\nu(\mathbf{r}+\mathbf{q})\phi_\lambda(\mathbf{r}+\mathbf{q}+\mathbf{u})$$
$$\times \phi_\sigma(\mathbf{r}+\mathbf{u})j_0(qv)d\mathbf{r}d\mathbf{q}d\Omega_u. \tag{15}$$

The evaluation of these integrals is the difficult step when computing intracules. For Gaussian basis functions, integrals involving basis functions of arbitrary angular momentum can be generated by the differentiation of the integral over four s-functions.[72] Position and momentum integrals can be expressed in terms of relatively simple closed form expressions. For the Wigner integrals no simple closed form expression could be found for the $[ssss]_W$ integral, consequently, the evaluation of these integrals is considerably more problematic. Two approaches were adopted, the first used quadrature, while the second expressed the integrals in terms of an infinite series.[63]

Intracules can then be generated through the two-particle density matrix. For HF wave functions, $\Gamma_{\mu\nu\lambda\sigma}$ can be expressed as

$$\Gamma_{\mu\nu\lambda\sigma}^{HF} = \tfrac{1}{2}[P_{\mu\nu}P_{\lambda\sigma} - P_{\mu\sigma}^\alpha P_{\nu\lambda}^\alpha - P_{\mu\sigma}^\beta P_{\nu\lambda}^\beta], \tag{16}$$

where $P_{\mu\nu}$, etc. are the HF density matrix elements. In our implementation, we follow the work of Maurice and Head-Gordon[73] for the construction of the CIS two-particle density matrix. $\Gamma_{\mu\nu\lambda\sigma}^{CIS}$ is expressed in terms of the HF density matrix, the CIS difference density matrix, and the atomic orbital representation of the CIS amplitudes. The CIS difference density matrix includes effects due to the relaxation arising from the use of HF orbitals in the CIS procedure. These matrices are evaluated and stored for all the excited states. For each batch of integrals evaluated, contraction with $\Gamma_{\mu\nu\lambda\sigma}^{CIS}$ is performed with the elements of $\Gamma_{\mu\nu\lambda\sigma}^{CIS}$ evaluated on the fly. Consequently, the storage of the four-index two-particle density matrix is not required. The relative cost of
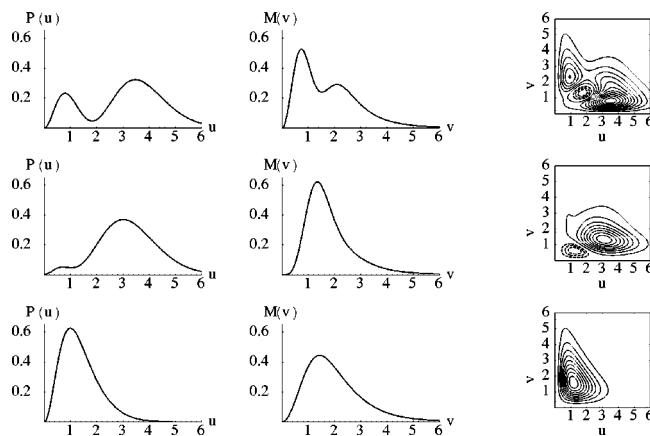

FIG. 1. Position, momentum, and Wigner intracules for He. Bottom row: ground state, middle row: $^3S(1s2s)$ state, top row: $^1S(1s2s)$ state. Negative contours are represented with broken lines.

this digestion of the integrals with the two-particle density matrix is small in comparison to the evaluation of the integrals. As a result, intracules for a number of states can be evaluated with little additional cost. This has been implemented within Q-Chem.[71]

III. INTRACULES FOR HE-LIKE IONS

Figure 1 shows the position, momentum, and Wigner intracules for the ground state and $^3S(1s2s)$ and $^1S(1s2s)$ states of He. The ground state intracule is generated at the HF level with the split-valence 6-31++G[74] basis set and the two excited states from the CIS/6-31++G wave function.[75] The ground state intracules have been discussed previously.[38,59] The momentum intracule is more diffuse than the position intracule and the Wigner intracule is positive everywhere and has one peak with a maximum at $(u,v) \approx (1.1,1.6)$. The intracules for the two excited states are strikingly different.

$P(u)$ intracules for He-like ions have been discussed in detail in the literature.[8,9,16,18,22,64] For the $^3S(1s2s)$ state, $P(u)$ is dominated by one peak whose maximum occurs at larger u than for the ground state. At the CIS level, the peak maximum moves from 1.1 au in the ground state to 3.2 au in the $^3S(1s2s)$ state. This illustrates the increased interelectron separation between electrons in the $1s$ and $2s$ orbitals. Near the origin, the intracules decay as u^4 instead of quadratically as seen for the ground state. This short-range behavior is related to the electron–electron cusp (this has been described in detail elsewhere[16,17]). $P(u)$ for the $^1S(1s2s)$ state is bimodal. The bimodal nature of $P(u)$ for the $^1S(1s2s)$ state has been observed previously in intracules derived from correlated wave functions.[9,64] In these intracules, the relative size of the two peaks differs from the CIS intracule presented here, with the peak at low u being considerably smaller than the peak at larger u. This may be a consequence of the uncorrelated nature of the CIS wave function, however, the relative size of the two peaks is also sensitive to the extent of the diffuse basis functions. This bimodal behavior has been attributed to the nodal structure of the wave function for this state.[16] The radial distribution
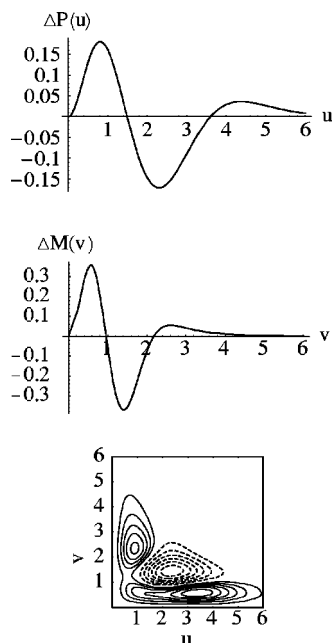
FIG. 2. He $^1S(1s2s)-^3S(1s2s)$ difference intracules. Negative contours are represented with broken lines.

FIG. 3. $^1S(1s2s)-^3S(1s2s)$ Wigner difference intracules for Be^{2+} (top), C^{4+} (middle), and Ne^{8+} (bottom). Negative contours are represented with broken lines.

function for the $2s$ orbital shows two distinct peaks. Consequently, electrons in the $2s$ orbital have a significant probability of being close to the nucleus as well as much further away. For $P(u)$ the peak at low u describes the interaction between the electrons in the $1s$ and $2s$ orbitals when the $2s$ electron is close to the nucleus, while the outer peak describes the $1s/2s$ interaction when the $2s$ electron is further from the nucleus. In general, the number of peaks in position intracule densities can be predicted from a screened hydrogenic model, although additional peaks at low u are found in S states.[22]

The momentum intracules for the $^3S(1s2s)$ and $^1S(1s2s)$ states have one and two peaks, respectively. However, for the singlet state the origin of the two peaks is reversed relative to its position space counterpart. The Wigner intracule has one large positive peak at (3.1,1.3). At low u and v there is a shallow negative region. This arises as a consequence of HF exchange which keeps electrons of the same spin apart. The small negative regions in Wigner intracules highlight the fact that the Wigner distribution can only be regarded as a "quasi probability distribution." For the $^1S(1s2s)$ state the Wigner intracule shows the two peaks clearly, with a small negative region in between. There is also significant intracule density at low u and v, since for CIS electrons of opposite spin are not correlated.

The effects of exchange are more clearly illustrated by the difference intracules $\Delta P(u) = P(u)(^1S(1s2s)) - P(u)(^3S(1s2s))$, and similarly for $\Delta M(v)$ and $\Delta W(u,v)$, which are shown in Fig. 2. $\Delta P(u)$ is qualitatively similar to corresponding intracules derived from more accurate wave functions.[16] However, there are differences in the relative size of the peaks. $\Delta P(u)$ shows clearly that there is a reduced probability of small u in the triplet state. This has been shown to be true for a large number of states.[22] This is what would be generally anticipated. There is also a greater
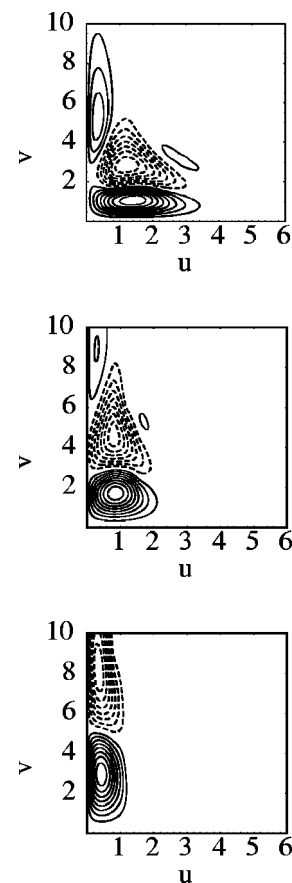
probability of large u in the singlet state. $\Delta M(v)$ has similar structure to $\Delta P(u)$. Consequently, there is also a reduced probability of low v in the triplet state. These changes are illustrated nicely by $\Delta W(u,v)$. In phase space there are two positive peaks at (1.0,2.3), (3.5,0.8); these represent the lower chance of finding electrons at small u and v in the triplet state, respectively. The negative peak at (2.5,1.5) shows an increase in moderate u and v in the triplet state.

For the He-like ions, $\Delta P(u)$ and $\Delta M(v)$ have qualitatively the same form. However, as the nuclear charge increases, $\Delta P(u)$ becomes more compact and $\Delta M(v)$ more diffuse. This reflects the smaller orbitals and greater speeds of the electrons as the nuclear charge increases. The corresponding $\Delta W(u,v)$ (Fig. 3) change significantly as nuclear charge increases. The three peaks remain but they are increasingly stretched in the v direction and squashed to low u.

IV. INTRACULES FOR BE-LIKE IONS

Figure 4 shows CIS/6-31+G (HF/6-31+G for the ground state) intracules for the singlet excited states of Be. The ground state intracule has been discussed in detail elsewhere.[38] The three peaks in the Wigner intracule arise from the $1s/1s$ (0.5,3.4), $1s/2s$ (2.1,2.3), and $2s/2s$ (2.9,0.8) interactions.

The intracules shown for Be are for excited states in which an excitation has occurred from the $2s$ orbital. Con-
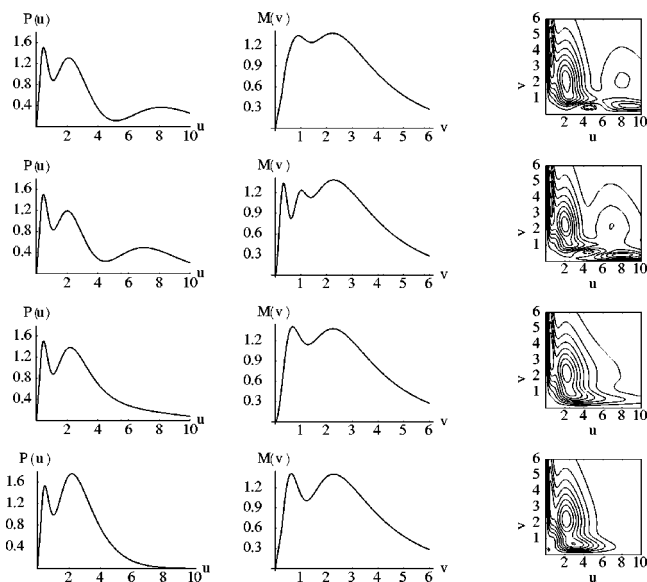
FIG. 4. Position, momentum, and Wigner intracules for the singlet states of Be. Bottom row: ground state, second row: $^1P(2s2p)$ state, third row: $^1S(2s3s)$ state, top row: $^1P(2s3p)$ state. Negative contours are represented with broken lines.

FIG. 5. Be $^1P(2s2p)-^3P(2s2p)$ difference intracules. Negative contours are represented with broken lines.

sequently, the peak describing the $1s/1s$ interaction should remain almost unchanged. The Wigner intracules confirm this. The location of the $1s/2s$ peak remains constant although the size of the peak decreases. As anticipated, most of the changes in the intracules are associated with the $2s/2s$ peak. For the intrashell excitation to the $2p$ orbital no new peaks can be distinguished in the intracules but there is a distinct elongation of the (2.9,0.8) peak in the u direction. This peak now corresponds to the $2s/2p$ interaction. For the intershell excitations to the $3s$ and $3p$ orbitals, distinct new peaks can be distinguished. This is a consequence of the $3s$ and $3p$ orbitals being considerably more diffuse. For the $^1S(2s3s)$ state, the new peaks at (7.0,2.0) and (8.0,0.3) correspond to the $1s/3s$ and $2s/3s$ interactions, respectively, and similarly the $1s/3p$ and $2s/3p$ interactions for the $^1P(2s3p)$ state.

The corresponding position intracules for these states show a well-defined shell structure. In particular, a third peak at large u is clearly seen for the $^1S(2s3s)$ and $^1P(2s3p)$ states. However, while three peaks can be seen in the momentum intracule for the $^1S(2s3s)$ state, for the $^1P(2s3p)$ state these peaks have begun to merge and only two can be distinguished.

Recently, difference intracules $^1P(2s2p)-^3P(2s2p)$ have been reported by Gálvez et al.[69] for the Be-like ions. These intracules showed some unexpected features. For Be, $\Delta P(u)$ is negative at low u and positive at high u. This suggests that the electrons tend to be closer in the triplet state than the singlet state. This is contrary to the common understanding of exchange, which should keep electrons of the same spin further apart. For the ions $C^{2+} \rightarrow Ne^{6+}$ the more expected result of positive and negative peaks at low and high u, respectively, was found. The corresponding $\Delta P(u)$, $\Delta M(v)$, and $\Delta W(u,v)$ for Be are shown in Fig. 5. Again, $\Delta P(u)$ has a negative region at low u. It is also long ranged,
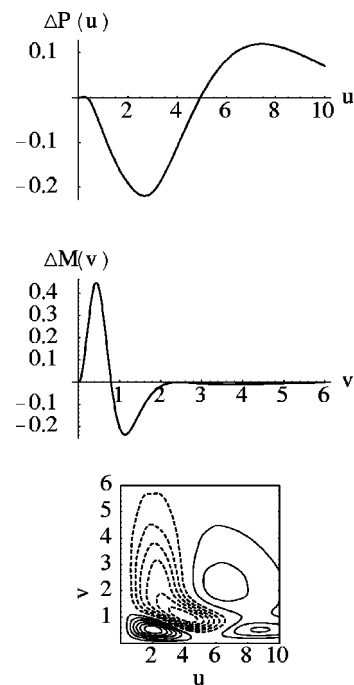
extending significantly to large u. $\Delta M(v)$ is shorter ranged and has a positive peak at low v suggesting, as expected, that low v is disfavored in the triplet state. A study of the Coulomb hole for Be, B^+, and C^{2+} also showed unexpected behavior for Be.[10] It was found that the average interelectronic separation between the $1s/2s$ and $2s/2s$ pairs decreased in the correlated wave function of the $^1P(1s2p)$ state. For B^+ and C^{2+} the introduction of correlation led to an increase in the interelectronic separations. The origin of this was found to be contraction of the $2p$ orbital in the $^1P(1s2p)$ state for Be. This contraction was not observed for the other ions.

The Wigner intracule can provide an alternative rationalization of these observations. Three regions are observed, two positive regions one with maxima at (2,0.5) and the other at high u and v. Between is a negative region. The peak at (2,0.5) indicates that in the triplet state electrons with low u and v are kept apart. However, in the singlet state electrons with low u and high v are more likely. This is physically reasonable since electrons already far apart in momentum space will be less affected by the introduction of exchange. Position intracules can be visualized as arising from projecting the Wigner intracule onto the u axis [Eq. (7)]. Consequently, the sign and magnitude of the peaks in $\Delta P(u)$ will depend on the delicate balance between these peaks. For Be the reduced chance of finding low u and low v in the triplet state is outweighed by an increase in low u and high v electrons and $\Delta P(u)$ is unable to distinguish between them. For the Be-like ions (Fig. 6), as the nuclear charge increases the tendency for the negative peak to reach beyond the positive peak at low u and low v decreases and consequently the first peak in $\Delta P(u)$ will be positive. This arises since the positive region extends to lower u as the nuclear charge increases. A physical interpretation of this is that in
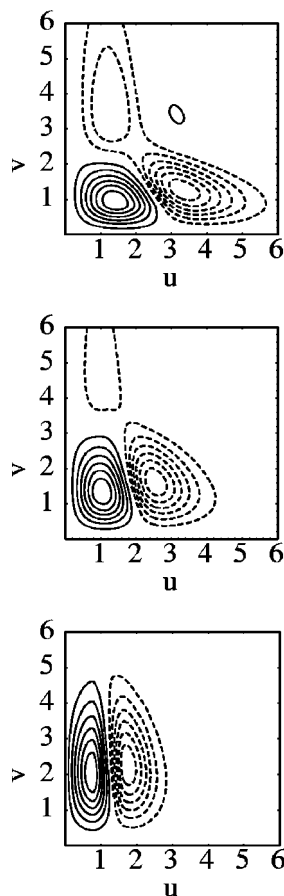
FIG. 6. $^1P(2s2p)-^3P(2s2p)$ Wigner difference intracules for B^+ (top), C^{2+} (middle), and O^{4+} (bottom). Negative contours are represented with broken lines.

Be a significant fraction of the electron density is sufficiently well separated in momentum space that introduction of exchange has little effect. However, in the ions the electrons are increasingly close in position space, and consequently, their relative separation in momentum space is not sufficient to compensate. The introduction of exchange correlation will then result in the electrons increasing their relative separations in the triplet state.

V. LARGER SYSTEMS

Intracules for formaldehyde are shown in Fig. 7 for the ground state (HF/6-31+G) and $^1n\pi^*$ and ^1n3s states (CIS/6-31+G). This provides an opportunity to compare intracules for valence and Rydberg states. Since we are primarily interested in changes in the electronic distribution upon electronic excitation, intracules for the excited states are represented as the difference in intracule densities (excited state-ground state).

The ground state intracules are typical of organic molecules. There is a distinct peak in $P(u)$ corresponding to the separation between heavy atoms and $M(v)$ is rather featureless with a long tail. The change in $P(u)$ indicates a general increase in the separation of the electrons in the excited states. This is particularly apparent for the ^1n3s state for which there is a large shift from low u to high u. This highlights the diffuse nature of the Rydberg orbital. The corre-
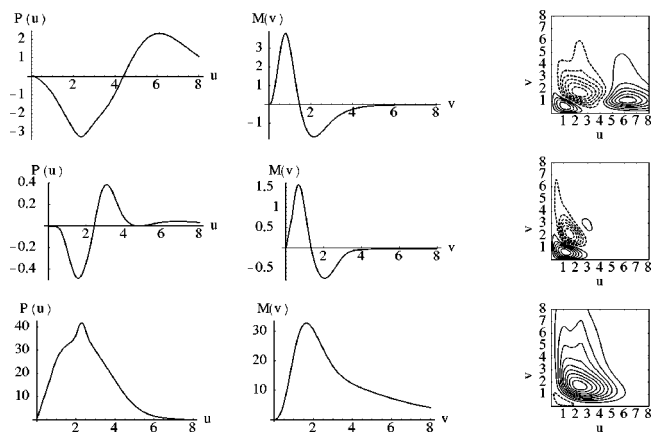

FIG. 7. Position, momentum, and Wigner intracules for formaldehyde. Bottom row: Ground state, middle row: change in intracule densities on excitation to the $^1n\pi^*$ state, top row: change in intracule densities on excitation to the ^1n3s state. Negative contours are represented with broken lines.

sponding momentum intracules of the two states have similar shapes. These intracules are considerably more short ranged than the position space counterparts. Both show a decrease in the relative momentum of the electrons. This is consistent with the electrons being excited to larger orbitals. The magnitude of the changes of relative position and momentum are significantly greater for the excitation to the Rydberg state. The Wigner intracules illustrate these features in more detail. For both states there is a small positive region at low u and low v, and a larger negative region at slightly higher u and v. The positive peak at low u and low v is unexpected, particularly for the ^1n3s state, since an electron is being excited to a more diffuse orbital. A possible explanation of its origin is that in addition to excitation to a more diffuse orbital, there is a contraction of the n orbital. For the ^1n3s state there is a further positive region at high u.

Figure 8 shows ground state intracules and changes in intracule densities for the $^1\pi\pi^*$ and $^1\pi3s$ states for butadiene, computed with the 6-31+G basis set. These intracules show similar trends observed for formaldehyde. In general, the change in intracule density is considerably more long
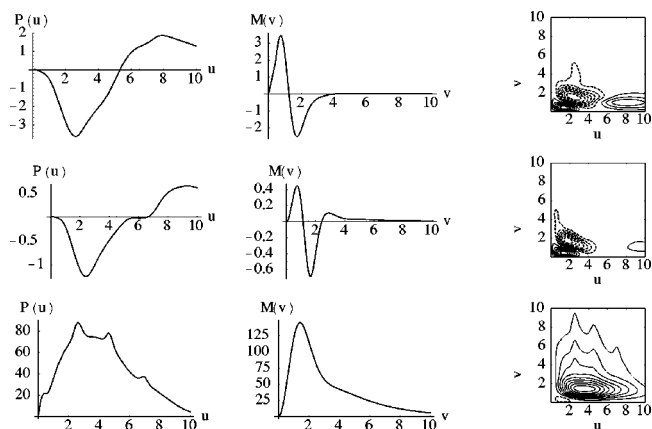

FIG. 8. Position, momentum, and Wigner intracules for butadiene. Bottom row: ground state, middle row: change in intracule densities on excitation to the $^1\pi\pi^*$ state, top row: change in intracule densities on excitation to the $^1\pi3s$ state. Negative contours are represented with broken lines.
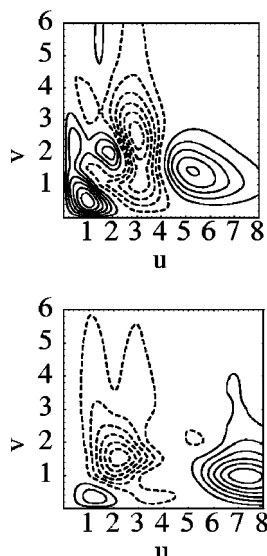
FIG. 9. Singlet–triplet Wigner difference intracules for formaldehyde, $n\pi^*$ state (top), $n3s$ state (bottom). Negative contours are represented with broken lines.

range in the u direction and is relatively short ranged in v. This is particularly true for the Rydberg state. Furthermore, the magnitude of the changes in the electronic distribution with respect to u and v is much larger for the excitation to the Rydberg state.

The difference in intracule densities between the singlet and triplet states of formaldehyde (Fig. 9) are more complex than for the atomic systems. However, both states have a similar qualitative pattern, with positive regions at low u and v and large u separated by a negative region. For the $n3s$ state, there are significant differences at large u and only a small peak at low u and v. For the $n\pi^*$ state, large differences occur at low u. Furthermore, significant changes are found at large v.

VI. CONCLUSIONS

In this article, the computation of position, momentum, and Wigner intracules for the CIS wave function has been described. Consequently, intracules for arbitrary excited states can be evaluated for atomic and molecular systems. Intracules provide valuable insight into the electronic distribution. In particular, the Wigner difference intracule provides a representation in phase space of changes that occur upon electronic excitation. For small systems, peaks in the intracules can often be associated with particular interelectron interactions. Excited state intracules for larger molecular systems have also been studied. These intracules show that changes in intracule density are more long ranged with respect to u than v. In particular, for excitations to Rydberg states the intracules show the significant increase in the relative separations of the electrons. Furthermore, the magnitude of the changes in intracule densities are larger for excitations to Rydberg states.

The effects of exchange on the electronic distribution are of fundamental interest, and have attracted considerable attention. These effects are ideally represented by the Fermi

hole, however, they can be studied through the difference in intracule density between singlet and triplet states. We have discussed such intracules in position, momentum, and phase space for a number of systems. We have found that a phase space representation is necessary for understanding and rationalization of these effects, in particular for the Be-like ions.

[1] A. S. Eddington, *Fundamental Theory* (Cambridge University Press, Cambridge, 1946).
[2] C. A. Coulson and A. H. Neilson, Proc. Phys. Soc. London **78**, 831 (1961).
[3] W. A. Lester, Jr. and M. Krauss, J. Chem. Phys. **41**, 1407 (1964).
[4] R. F. Curl and C. A. Coulson, Proc. Phys. Soc. London **85**, 647 (1965).
[5] A. J. Coleman, Int. J. Quantum Chem. **1S**, 457 (1967).
[6] K. E. Banyard and C. C. Baker, J. Chem. Phys. **51**, 2680 (1969).
[7] R. Banesch and V. H. Smith, Jr., Acta Crystallogr., Sect. A: Cryst. Phys., Diffr., Theor. Gen. Crystallogr. **26**, 586 (1970).
[8] J. Katriel, Phys. Rev. A **5**, 1990 (1972).
[9] R. J. Boyd and C. A. Coulson, J. Phys. B **6**, 782 (1973).
[10] H. Tatewaki and K. Tanaka, J. Chem. Phys. **60**, 601 (1974).
[11] E. A. Colbourn, J. Phys. B **8**, 1926 (1974).
[12] A. J. Thakkar and V. H. Smith, Jr., Chem. Phys. Lett. **42**, 476 (1976).
[13] A. J. Thakkar and V. H. Smith, Jr., J. Chem. Phys. **67**, 1191 (1977).
[14] K. E. Banyard and P. K. Youngman, J. Phys. B **15**, 853 (1982).
[15] A. J. Thakkar, A. N. Tripathi, and V. H. Smith, Jr., Int. J. Quantum Chem. **26**, 157 (1984).
[16] P. E. Regier and A. J. Thakkar, J. Phys. B **17**, 3391 (1984).
[17] A. J. Thakkar, J. Chem. Phys. **84**, 6830 (1986).
[18] A. J. Thakkar, J. Phys. B **20**, 3939 (1987).
[19] R. J. Boyd, C. Sarasola, and J. M. Ugalde, J. Phys. B **21**, 2555 (1988).
[20] J. M. Ugalde, C. Sarasola, L. Dominguez, and R. J. Boyd, J. Math. Chem. **6**, 51 (1991).
[21] J. Wang, A. J. Thakkar, and V. H. Smith, Jr., J. Chem. Phys. **97**, 9188 (1992).
[22] N. M. Cann, R. J. Boyd, and A. J. Thakkar, J. Chem. Phys. **98**, 7132 (1993).
[23] K. E. Banyard and D. R. T. Keeble, J. Phys. B **27**, 5453 (1994).
[24] J. Wang and V. H. Smith, Jr., Int. J. Quantum Chem. **49**, 147 (1942).
[25] J. Cioslowski, J. Stefanov, A. Tang, and C. J. Umrigar, J. Chem. Phys. **103**, 6093 (1995).
[26] J. Cioslowski and G. Liu, J. Chem. Phys. **105**, 4151 (1996).
[27] J. Cioslowski and G. Liu, J. Chem. Phys. **109**, 8225 (1998).
[28] T. Koga and H. Matsuyama, J. Phys. B **31**, 3765 (1998).
[29] X. Fradera, C. Sarasola, J. M. Ugalde, and R. J. Boyd, Chem. Phys. Lett. **304**, 393 (1999).
[30] T. Koga, H. Matsuyama, J. S. Dehesa, and A. J. Thakkar, J. Chem. Phys. **110**, 5763 (1999).
[31] T. Koga and H. Matsuyama, J. Chem. Phys. **111**, 9191 (1999).
[32] F. J. Gàlvez, E. Buendìa, and A. Sarsa, J. Chem. Phys. **111**, 10903 (1999).
[33] A. M. Lee and P. M. W. Gill, Chem. Phys. Lett. **313**, 271 (1999).
[34] X. Fradera, M. Duran, and J. Mestres, J. Phys. Chem. A **104**, 8445 (2000).
[35] P. M. W. Gill, A. M. Lee, N. Nair, and R. D. Adamson, J. Mol. Struct.: THEOCHEM **506**, 303 (2000).
[36] E. Valderrama, X. Fradera, and J. M. Ugalde, J. Chem. Phys. **115**, 1987 (2001).
[37] E. Valderrama and J. M. Ugalde, Int. J. Quantum Chem. **86**, 40 (2002).
[38] P. M. W. Gill, D. P. O'Neill, and N. A. Besley, Theor. Chem. Acc. **109**, 241 (2003).
[39] K. E. Banyard and C. E. Reed, J. Phys. B **11**, 2957 (1978).
[40] C. E. Reed and K. E. Banyard, J. Phys. B **13**, 1519 (1980).
[41] R. J. Mobbs and K. E. Banyard, J. Chem. Phys. **78**, 6106 (1983).
[42] P. K. Youngman and K. E. Banyard, J. Phys. B **20**, 3313 (1987).
[43] J. M. Ugalde, J. Phys. B **20**, 2153 (1987).
[44] K. E. Banyard and P. K. Youngman, J. Phys. B **20**, 5585 (1987).

[45] K. E. Banyard, K. H. Al-Bayati, and P. K. Youngman, J. Phys. B **21**, 3177 (1988).

[46] K. E. Banyard and R. J. Mobbs, J. Chem. Phys. **88**, 3788 (1988).

[47] K. E. Banyard and J. Sanders, J. Chem. Phys. **99**, 5281 (1993).

[48] J. Wang and V. H. Smith, Jr., J. Chem. Phys. **99**, 9745 (1993).

[49] D. R. T. Keeble and K. E. Banyard, J. Phys. B **30**, 13 (1997).

[50] T. Koga and H. Matsuyama, J. Chem. Phys. **107**, 8510 (1997).

[51] H. Matsuyama, T. Koga, E. Romera, and J. S. Dehesa, Phys. Rev. A **57**, 1759 (1998).

[52] T. Koga and H. Matsuyama, J. Chem. Phys. **111**, 643 (1998).

[53] H. Matsuyama, T. Koga, and Y. Kato, J. Phys. B **32**, 3371 (1998).

[54] T. Koga and H. Matsuyama, J. Chem. Phys. **113**, 10114 (2000).

[55] T. Koga, Y. Kato, and H. Matsuyama, Theor. Chem. Acc. **106**, 237 (2001).

[56] T. Koga, Chem. Phys. Lett. **350**, 135 (2001).

[57] T. Koga, J. Chem. Phys. **116**, 6614 (2002).

[58] T. Koga, Theor. Chem. Acc. **107**, 246 (2002).

[59] N. A. Besley, A. M. Lee, and P. M. W. Gill, Mol. Phys. **100**, 1763 (2002).

[60] E. Wigner, Phys. Rev. **40**, 749 (1932).

[61] M. Hillery, R. F. O'Connell, M. O. Scully, and E. P. Wigner, Phys. Rep. **106**, 121 (1984).

[62] M. Springborg and J. P. Dahl, Phys. Rev. A **36**, 1050 (1987).

[63] N. A. Besley, D. P. O'Neill, and P. M. W. Gill, J. Chem. Phys. **118**, 2033 (2003).

[64] D. A. Kohl, J. Chem. Phys. **56**, 4236 (1972).

[65] J. M. Mercero, J. M. Elorza, J. M. Ugalde, and R. J. Boyd, Phys. Rev. A **60**, 4375 (1999).

[66] R. J. Boyd and C. A. Coulson, J. Phys. B **14**, 1805 (1974).

[67] R. P. Messmer and F. W. Birss, J. Phys. Chem. **73**, 2085 (1969).

[68] N. Moiseyev and J. Katriel, Chem. Phys. **10**, 67 (1975).

[69] F. J. Gàlvez, E. Buendìa, and A. Sarsa, J. Chem. Phys. **118**, 6858 (2003).

[70] P. M. W. Gill, D. P. O'Neill, and N. A. Besley (unpublished).

[71] J. Kong, C. A. White, A. I. Krylov *et al.*, J. Comput. Chem. **21**, 1532 (2000).

[72] S. F. Boys, Proc. R. Soc. London, Ser. A **200**, 542 (1950).

[73] D. Maurice and M. Head-Gordon, Mol. Phys. **96**, 1533 (1999).

[74] W. J. Hehre, R. Ditchfield, and J. A. Pople, J. Chem. Phys. **56**, 2257 (1972).

[75] The exponent of the diffuse function in the 6-31++G basis for H is 0.036, so we have used a diffuse function exponent of $(27/16)^2 \times 0.036$ for He.